Short-Wavelength Collective Dynamics in Metastable Water A Molecular Dynamics Simulation Study

Th. Kowall, P. Mausbach, and A. Geiger

Physikalische Chemie, Fachbereich Chemie der Universität Dortmund, Postfach 50 05 00, D-4600 Dortmund 50

Institut für Physikalische Chemie, RWTH Aachen, Templergraben 59, D-5100 Aachen

Collective Dynamics / Computer Experiments / Hydrogen-Bond Network / Simulation / Water

Motivated by a controversial discussion of the short-wavelength collective dynamics in water, we calculate the coherent dynamic structure factor from the oxygen motion in low-density water. In accord with early results of Rahman and Stillinger, we detect at the lowest accessible wavevectors the simultaneous existence of two Brillouin lines. Whereas the low-frequency mode is strongly damped and is considered to be a remnant of the ordinary sound, the high-frequency mode can be attributed to collective excitations, propagating within the hydrogen-bond network. Consequently, a density decrease lowers the weak damping of this mode even more, due to the increasing rigidity of the hydrogen-bond network. For comparison, we also discuss the temperature and density dependence of a related single particle property, the frequency spectrum of the velocity autocorrelation function.

1. Introduction

Long-wavelength density fluctuations in fluids have been studied extensively by theory and experiment. In classical hydrodynamics they can be described by a few transport coefficients and thermodynamic properties of the material [1–3]. Much less clear is the physical nature of collective excitations (sound modes) at short wavelengths, that means in the region of a few molecular diameters, where a continuum approach is no more valid. At these wavelengths the lifetime of a propagating mode is strongly damped by the self motion of the single particles. This makes it very difficult to detect experimentally the corresponding Brillouin peaks in the presence of the strong quasielastic central line. A theoretical description of these density fluctuations has to include the specific interaction potential. This has been achieved in generalized hydrodynamics only for simple fluids in an approximative manner (using parametrized memory functions or a kinetic equations approach [1, 2]).

At this stage, molecular dynamics (MD) simulations can be used as a tool to elucidate the connections between manybody dynamics and interaction potentials. One of the important advantages of this method is the possibility to study systems in modified, even in experimentally not accessible states, to reveal the underlying physical mechanisms.

Short-wavelength excitations can be detected experimentally as Brillouin-lines in the dynamic structure factor $S(q,\omega)$ from coherent inelastic neutron scattering. This has been achieved until now for a few atomic liquids only: rubidium [4], lead [5] and neon [6]. In these cases, the observed collective mode is considered to be a remnant of the hydrodynamic sound mode, which shows an extraordinarily weak damping due to the peculiarities of the interatomic potentials with a smooth repulsion and a strong attractive well.

2. Summary of Previous Results

2.1. Collective Dynamics in Water

In 1974 an analysis of the density fluctuations in water yielded a very surprising result. Evaluating their famous MD simulation of water, Rahman and Stillinger detected *two* Brillouin-like maxima in the spectrum of density fluctuations [7]. The low frequency one could be attributed to the ordinary sound, exhibiting a velocity of about 1800 m/s. The second, high-frequency maximum, which showed a roughly doubled velocity of propagation, had to be assigned to a novel excitation.

Subsequent light- and neutron-scattering experiments on water at first sight yielded divergent results. In both cases, only *one* Brillouin band could be detected, and the extracted velocities of propagation differed markedly: whereas in the light-scattering experiment the ordinary sound speed was observed [8], neutron-scattering yielded a velocity which was in agreement with the *high frequency* mode of Rahman and Stillinger [9]. This was explained as follows: light-scattering cannot detect the high frequency excitation, because this is propagating within clusters of strongly hydrogen-bonded water molecules, which extend over only a few Angstrom [10, 11]. On the other hand, the neutron scattering experiment had difficulties to observe the ordinary sound, because of a limited resolution, but mainly because of the expected strong damping of this mode at high wavevectors.

Subsequent simulations of water on the basis of MCY [12, 13] and TIP4P [14] interaction potentials were not considered as to confirme the outlined interpretation. Particularly, no two different Brillouin-like bands could be observed. In all cases, the authors could trace only *one* mode in $S(q,\omega)$ with a velocity of propagation of about 3000 m/s. Consequently, this mode was interpreted as being the manifestation of the hydrodynamic sound in the region of small wavelengths. In this case, the high speed of propagation must be due to an appreciable positive dispersion. Moreover, an unusually low damping must be in action.

In a very recent study of Ricci et al. [15] yet a new point is added to the discussion: these authors observed again two distinct excitations, one in the oxygen dynamic structure factor, which is comparable to the feature in the MD simulations of Refs. [12, 13] and also interpreted correspondingly. The second one is present in the hydrogen density correlation function only, at extremely high frequencies ($\omega \approx$ 100 to 160 THz), comparable to the frequency of the small-angle hindered rotations ("librations") of the water molecules.

Ber. Bunsenges. Phys. Chem. *94*, 279–285 (1990)
0005–9021/90/0303–0279 $ 02.50/0

It should be mentioned here that Bosse et al. [16] also report the observation of a "fast sound". In their computer simulation of liquid $Li_{0.8}Pb_{0.2}$ a new high-frequency and short-wavelength collective mode with high propagation velocity and weak damping is appearing. However, in this case this fast motion entails the motion of the light atoms only, whereas in water the fast mode (compared to the ordinary sound speed) has been observed from oxygen or center-of-mass motion.

In view of the outlined controversial results and interpretations, we aimed at reproducing the old Rahman-Stillinger results from a *direct* calculation of the coherent dynamic structure factor $S(q,\omega)$, i.e. without the memory function extrapolation procedure used by these authors. Additionally, we study the influence of a density variation. As we set out in the following section, a density decrease produces a strengthening of the hydrogen-bond network in water. Therefore a less damped, more "solid-like" propagation of those excitations, which are mediated by the H-bond network is expected in "stretched" water. On the other hand, the associated increase of the viscosity should produce an amplified decay of the "ordinary" sound propagation.

2.2. Hydrogen-bond Network and Density Fluctuations in Ordinary Water

Various models of water which attempt to explain its anomalous properties are based on the capability of water to form a quasi "infinite" three-dimensional random network of H-bonds [17, 18]. The importance of small enclosed regions of strongly connected water molecules for the unusual thermodynamic and structural properties of water has been discussed in detail [19, 20]. Therefore it is natural to conjecture a similar significance of such ("ice-like") clusters for the collective dynamics. In particular, it seems to be reasonable to link the high velocity of excitation and low, solid-like damping of the short-wavelength excitations with the existence of these ramified clusters of strongly connected water molecules. The small extension of such "locally-structured" regions of a few Angstrom could easily explain the fact that this mode could not be detected in light scattering experiments.

2.3. Simulation of Stretched Water

The properties of metastable (supercooled, superheated, stretched) water and its limits of mechanical stability were in the center of various studies during the last years [21]. To elucidate the structural and microdynamical changes which occur on the approach of the limits, two extensive series of simulation runs were produced in our group [18, 22, 23], one at constant temperature ($T \approx 271$ K) and decreasing density (from $\varrho = 1.0$ to 0.7 g/cm^3), the other at constant density ($\varrho = 1.0$ g/cm^3) and varying temperature (from $T = 287$ K to 235 K). In contrast to the "normal" behavior of liquids, but in agreement with the behavior expected from high pressure experiments [24], we observed a very strong decrease of the single particle mobility with decreasing density. The mobility extrapolates to zero at roughly 0.8 g/cm^3, which is the density at the conjectured limit of mechanical stability for stretched water [25].

This density dependence of the mobility is caused by a change in the H-bond network structure, that has been characterized as follows: at 1.0 g/cm^3 water consists of a continuous random "tetrafunctional" network with many local defects like "bifurcated H-bonds" [18, 26, 27]. These defects are essential for the mobility of the water molecules. With decreasing density an "ideal" tetrafunctional network, comparable to the random network models of amorphous semiconductors, like the Polk model [28], is approached [18, 29]. (In the picture of the previous section 2.2, these structural changes have to be described as an increase of the more structured clusters.) In this highly viscous, more gel-like state, the single molecule mobility is decreased as described above, but moreover one expects a less damped, more solid-like behavior of collective excitations, which are transmitted through the H-bond network.

3. Method

3.1. Outline of the MD Simulations

In a preliminary test we used coordinate sets from the previous MD simulation series, mentioned in section 2.3. Unfortunately, the recorded trajectories of about 10 ps did not yield sufficient statistical accuracy. Therefore we produced new runs of 140 ps each, corresponding to about 115000 timesteps, at constant energies and densities. These long runs at densities of 0.95 and 0.85 g/cm^3 and a temperature of about 275 K are the basis of the following results.

In accord with the study of Rahman and Stillinger [7], our system consists of 216 water molecules, which interact via the ST2 potential. To reduce computer time, we proceed as in previous studies [22, 23]: the interaction cutoff is set to 7.8 Å and combined with a reaction field approximation [30].

3.2. Definitions

Collective dynamics in a many particle system is described by the coherent dynamic structure factor, which is the space-time Fourier transform of the density autocorrelation function [1]. In detail, if

$$\varrho(\boldsymbol{r},t) = \sum_{i=1}^{N} \delta(\boldsymbol{r} - \boldsymbol{r}_i(t)) \tag{1}$$

is the microscopic number density and

$$\varrho_q(t) = \int \varrho(\boldsymbol{r},t) \cdot \mathrm{e}^{-i\boldsymbol{q}\boldsymbol{r}}\, \mathrm{d}\boldsymbol{r} = \sum_{i=1}^{N} \mathrm{e}^{-i\boldsymbol{q}\boldsymbol{r}(t)} \tag{2}$$

its Fourier transform, the corresponding time autocorrelation function

$$F_{\mathrm{coh}}(|\boldsymbol{q}|,t) = \frac{1}{N} \langle \varrho_q(t) \cdot \varrho_q^*(0) \rangle_{|\boldsymbol{q}|} \tag{3}$$

is called the coherent intermediate scattering function. Note that in the present study we concentrate on the oxygen dynamics, therefore all position vectors $\boldsymbol{r}_i(t)$ refer to oxygen positions. In Eq. (3) the isotropy of the liquid is taken into

account by averaging not only over the whole time sequence, but also over all wavevectors $\boldsymbol{q}$ with the same magnitude $|\boldsymbol{q}|$. The wavevectors $\boldsymbol{q}$ have to be chosen in accord with the periodic boundary conditions:

$$\boldsymbol{q} = \frac{2\pi}{L}(n_x, n_y, n_z)$$

with integer n_x, n_y and n_z and L being the cube edge of the periodic box. Accordingly, the smallest accessible $|q|$-values are 0.3374, 0.3316 and 0.3196 Å^{-1} for the three different densities.

By transforming $F_{\text{coh}}(|\boldsymbol{q}|, t)$, the coherent dynamic structure factor is obtained:

$$S_{\text{coh}}(|\boldsymbol{q}|, \omega) = \frac{1}{2\pi}\int F_{\text{coh}}(|\boldsymbol{q}|, t)\, \mathrm{e}^{-i\omega t}\, \mathrm{d}t\,. \tag{4}$$

Starting from the oxygen positions $\boldsymbol{r}_i(t)$, as obtained by the MD simulation, the calculation of $F_{\text{coh}}(q,t)$ is straightforward. This can be achieved either by conventional techniques [31] or by applying the fast correlation algorithm, based on the Wiener-Khinchin theorem, as it is done in the data analysis program of Kneller [32], which we use.

Because we are interested in faint contributions to $S_{\text{coh}}(q,\omega)$, the Fourier transformation (4) has to be done with special care, to avoid any artifacts, especially truncation effects due to the slow decay of $F_{\text{coh}}(q,t)$ as well as "backfolding" of noise.

4. Results

4.1. The Intermediate Scattering Function $F_{\text{coh}}(q,t)$

Fig. 1a–c shows the intermediate coherent scattering function $F_{\text{coh}}(q,t)$ for the densities ϱ = 1.0, 0.95 and 0.85 g/cm^3 and for the smallest accessible wavevectors $\boldsymbol{q}$. Also, the smoothed function, as used for the Fourier transformation and the corresponding spectra (inserts) are given.

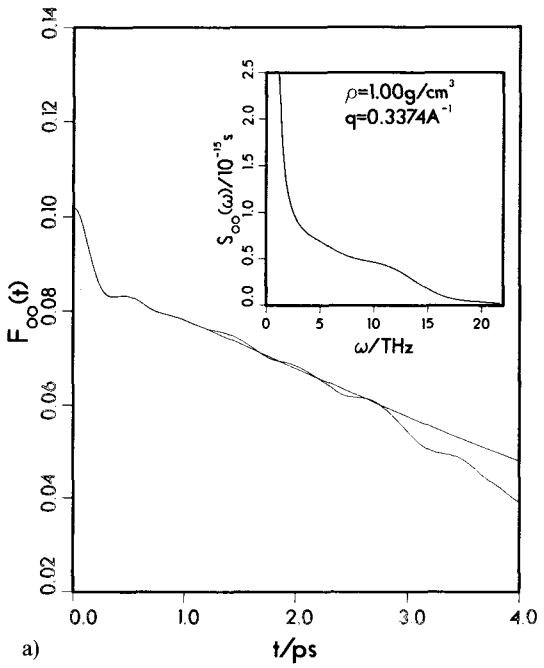

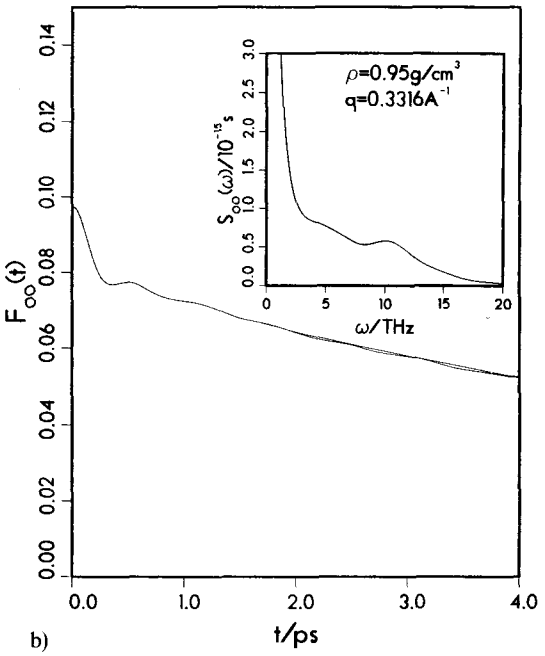

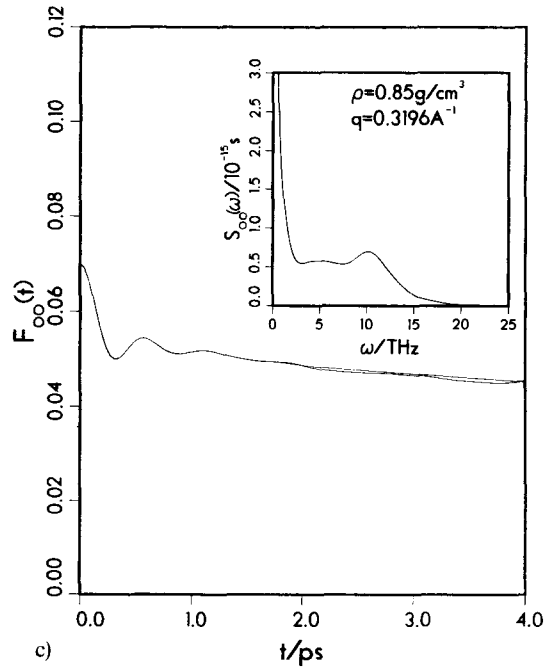

Fig. 1
Intermediate coherent dynamic scattering functions at the lowest accessible wavevectors and spline function extrapolation curves, used for the Fourier transformation to get the dynamic structure factors in the inserts. Temperature is close to 273 K

The collective dynamics is characterized by two different mechanisms with separate time scales. At long times, $F_{\text{coh}}(q,t)$ is dominated by an exponential decay, which reflects the decay of spatial correlations by diffusive, non-directed fluctuations. Propagating density fluctuations, which are periodic in space and time, are seen in $F_{\text{coh}}(q,t)$ as strongly damped oscillations at short times. It is essential that these oscillations gradually merge into the increasing statistical noise at large times (t > 1.0 to 1.5 ps). This inevitably demands smoothing before Fourier transformation,

as Fourier transformation expects high accuracy in the whole time range. Otherwise the noise in the time domain leads to an appreciable worsening of signal-to-noise ratio in the whole spectral range. Moreover, as $F_{coh}(q,t)$ is a slowly decaying function, which does not reach zero within the simulation time, some kind of smooth extension of the initial part is necessary. Such a procedure is certainly not fully straightforward and not free of some empiricism.

What can already be seen in the time domain, is a decrease of the damping in the short time oscillations of $F_{coh}(q,t)$, when the global density is decreased.

4.2. The Dynamic Structure Factor $S(q,\omega)$

There remains the problem to detect possibly two damped Brillouin-peaks next to a quasielastic band with an intensity which is two to three orders of magnitude higher. This demands a very high quality of the time correlation functions and requires long simulation runs. If we assume a ratio of 1:2 for the Brillouin-peak frequencies, the low-frequency mode appears in the time correlation function as a not very pronounced modulation of the decaying high-frequency oscillations. Hence, a reliable identification of two Brillouin-peaks is seriously hampered, if the oscillations are submerged in the noise, before they have decayed. Also, a smoothing extrapolation of the time correlation function is important, to reduce truncation effects and spurious lines in the frequency spectrum.

Smoothing by Gauss-windows is not appropriate here, because a maximum resolution is striven for [32]. Also, an extrapolation by fitting to an autoregressive (AR) model, as applied by Wojcik and Clementi [13], did not prove to be reliable. AR-models have difficulties, when the intensity ratios between the various lines are as large as in our case.

Motivated by a paper of Wormeester et al. [33], B-spline functions were used for a smooth and structureless extrapolation of the intermediate scattering functions. The 2^N data-points for fast Fouriertransformation were gained then by ordinary cubic spline interpolation. Of course, this procedure is justified only, if the oscillatory decay has faded away, before the extrapolation function sets in.

As the insert of Fig. 1a shows, at $\varrho = 1.0$ g/cm^3 no peaks can be resolved, but a shoulder structure indicates already the existence of two independent Brillouin-lines, as they appear more clearly at the lower densities in Figs. 1b and 1c. Yet, apparently this clearer resolution is not produced by a more pronounced peak at $\omega \approx 5$ THz, but by a slight narrowing of the neighbouring lines.

As we will see later from Fig. 4a, at least for the high-frequency (HF) mode it is reasonable to apply a linear dispersion relation to extract a speed of propagation

$$c = \frac{\omega}{q}. \tag{5}$$

If we do so for the low frequency (LF) peak in Figs. 1b and c, we find a sound velocity $c_l \approx 1500$ m/s. This confirms the observation of Rahman and Stillinger; they give the value 1800 m/s for $\varrho = 1.0$ g/cm^3 and $T = 283$ K. The shift to lower values in our simulations is in accord with measurements of the sound velocity c_s in supercooled water by light scattering [8]. c_s decreases with decreasing temperature, analoguous to the anomalous temperature dependence of the isothermal compressibility.

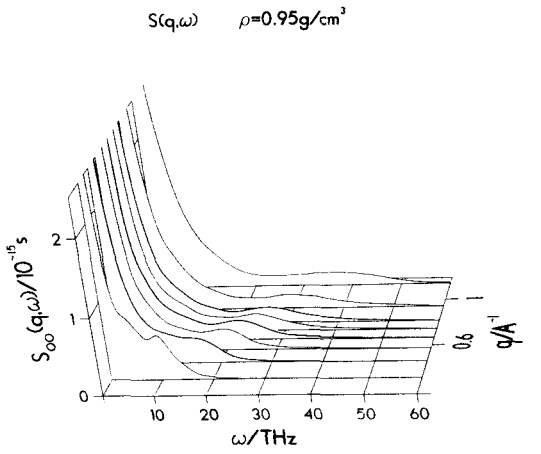

Fig. 2
Coherent dynamic structure factor $S(q,\omega)$ for different wavevectors q at the density $\varrho = 0.95$ g/cm^3 and temperature $T = 275$ K

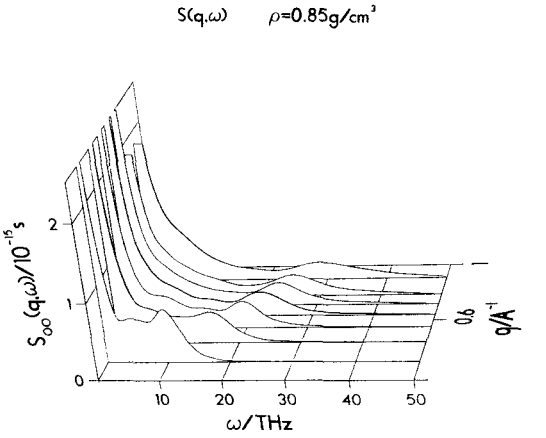

Fig. 3
Same as Fig. 2, for the density $\varrho = 0.85$ g/cm^3

In Figs. 2 and 3 $S(q,\omega)$ is shown for several q-values up to about 1 Å^{-1} and for the two densities $\varrho = 0.95$ and 0.85 g/cm^3. The LF mode quickly disappears in the broadening central line, whereas the HF mode persists up to the highest q-values. Most important, the HF mode becomes more intense with decreasing density, which is contradictory to the hydrodynamic relation between sound absorption and viscosity (the density decrease lowers the single particle mobility [18, 23] and hence increases the viscosity, which in turn should lead to a stronger damping).

On the other hand, the observed behavior is in agreement with the idea that the HF excitation is transmitted through the H-bond network, which becomes "stiffer" at lower densities. Fig. 5 gives the "full-width at half maximum (FWHM)" of this mode, measured on the high frequency side of the peak and assuming a symmetric line. Although these values are furnished with large error bars, the width,

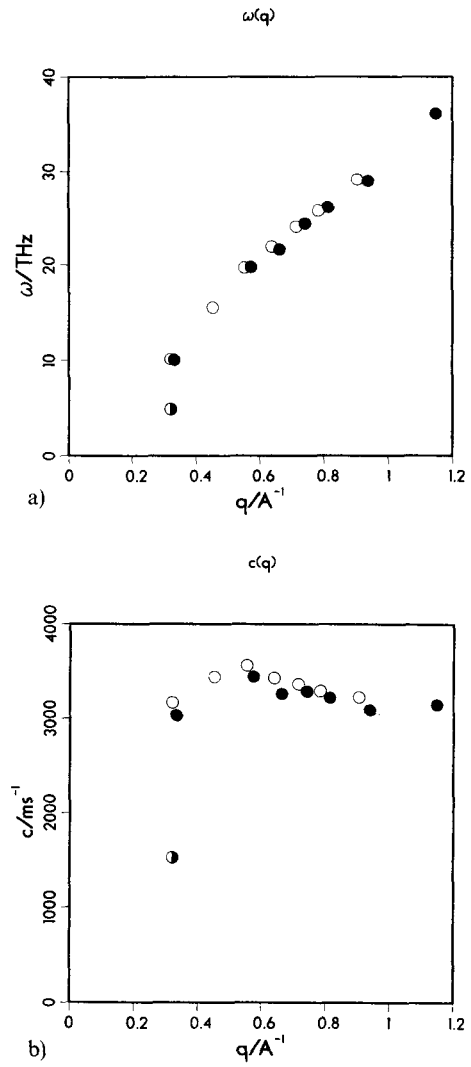

Fig. 4
a) Positions of the high-frequency Brillouin lines in $S(q,\omega)$ for $\varrho = 0.95$ g/cm^3 (●) and $\varrho = 0.85$ g/cm^3 (○). ◑: position of the low-frequency peak at $\varrho = 0.85$ g/cm^3
b) Corresponding velocities of propagation $c(q)$

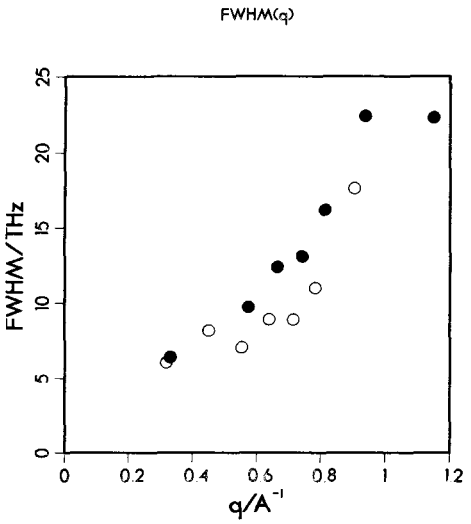

Fig. 5
"Full-width at half maximum" of the high-frequency Brillouin line for $\varrho = 0.95$ g/cm^3 (●) and $\varrho = 0.85$ g/cm^3 (○)

and with that the attenuation is systematically lower at $\varrho = 0.85$ g/cm^3.

The dispersion $\omega(q)$, as given in Fig. 4a is rather linear. This yields in Fig. 4b a more or less constant velocity of propagation upon application of Eq. (5). Moreover, Fig. 4b indicates an independence (or extremely weak dependence) of the HF sound velocity from the density.

4.3. Single Particle Dynamics in Stretched Water

To support our findings on the collective dynamics, we report some results concerning the single-particle dynamics, obtained from the previous simulation series on metastable water (see section 2.3). These single-particle properties provide a much better statistical accuracy, compared with the collective properties.

The dynamics of the H-bond network in supercooled water has also been studied by the measurement of Raman spectra [34]. Two characteristic bands at $\nu_2 = 190$ cm^{-1} and $\nu_1 = 60$ cm^{-1} had been attributed to intermolecular O–O-stretching and to intermolecular O–O–O-bending motions of H-bonded water molecules. With decreasing temperature ν_2 is shifted to higher frequencies, whereas ν_1 is practically temperature independent.

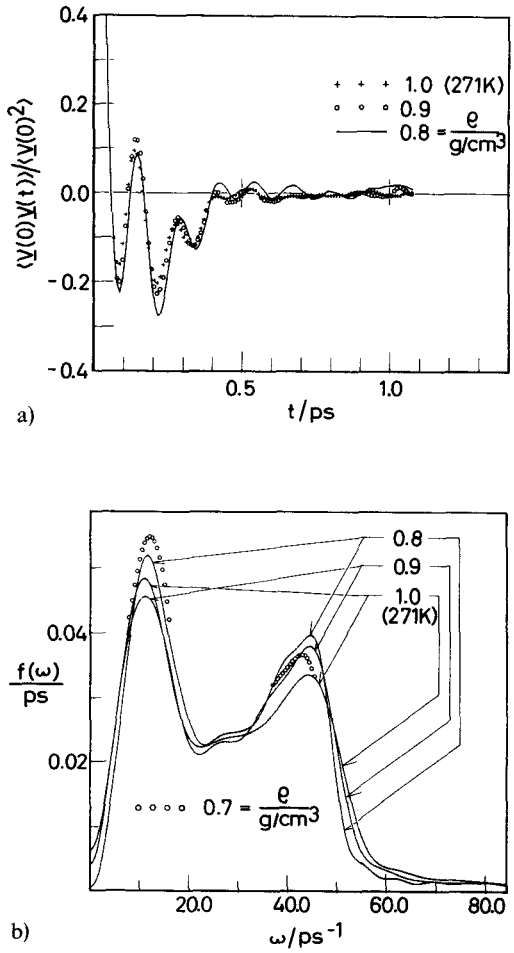

Fig. 6
a) Velocity autocorrelation functions $c_v(t)$ of the oxygen motion at different densities,
b) corresponding spectra $f(\omega)$

We compare this behavior with the velocity autocorrelation function (vacf)

$$c_v(t) = \langle \boldsymbol{v}(t_0) \cdot \boldsymbol{v}(t_0 + t) \rangle \tag{6}$$

of the oxygens and its frequency spectrum $f(\omega)$. In Fig. 6a $c_v(t)$ is given for different densities. The shape of $c_v(t)$ can be interpreted as the superposition of two damped oscillations. The low-frequency part is comparable to the vacf in simple liquids: a fast initial decay of the correlation is followed by a large negative region. This course is due to the motion of the molecules in the cage of its neighbors. The change of sign is produced by the reversal of the velocities after the collision with the "wall" of the cage. The strong damping of the oscillations indicates the short lifetime of the cage. This "ordinary" shape of the vacf is superimposed by much less damped high-frequency oscillations, which are due to the intermolecular motion of H-bonded molecules.

Accordingly, the frequency spectra $f(\omega)$ (Fig. 6b) show two pronounced maxima. The LF peak at $\omega \approx 11 \cdot 10^{12}$ $s^{-1} \approx 60$ cm^{-1} coincides with the Raman band attributed to the O–O–O bending motion. Also, the very weak temperature and density dependence of the peak position (Fig. 7) is in agreement with the experimental findings [34]. The assignment of this frequency to the motion in the cage of neighbors, as suggested by the simulation, includes the special case of an intermolecular bending motion.

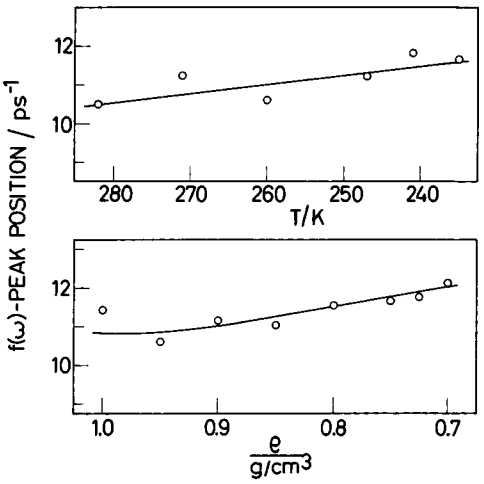

Fig. 7
Position of the low-frequency peak in the vacf spectra $f(\omega)$,
a) temperature dependence at constant density $\varrho = 1.0$ g/cm^3,
b) density dependence at constant temperature $T \approx 273$ K

The HF peak in $f(\omega)$ at $\omega \approx 44 \cdot 10^{12}$ $s^{-1} \approx 230$ cm^{-1} is shifted to higher frequencies in comparison with the Raman bands (this is expected from the known deficits of the ST2 potential, which overemphasizes the strength of the H-bonds). In agreement with the Raman-spectra, this peak shows a drift to higher frequencies with decreasing temperature (Fig. 8a; the corresponding $f(\omega)$ can be found in [35]). On the other hand, with decreasing density there is no pronounced shift of the positions (Fig. 8b), but a marked decline of the damping (Fig. 6b). These findings parallel the discussed dependencies of the collective excitations and also indicate a "stiffening" of the H-bond network (the final decrease of the frequencies in Fig. 8b is due to the rupture of the network beyond $\varrho = 0.8$ g/cm^3).

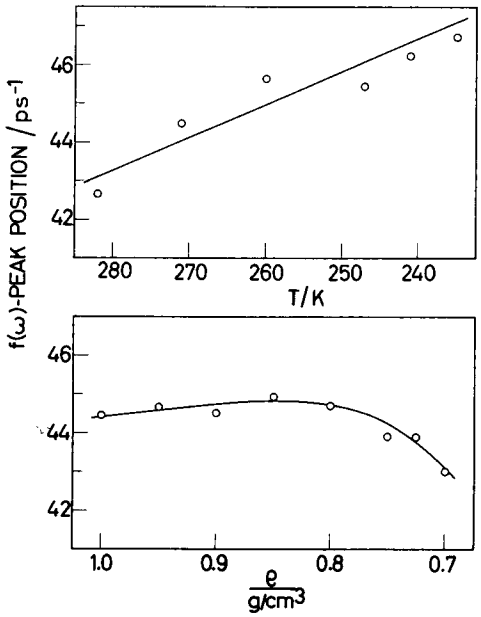

Fig. 8
Same as Fig. 7, for the high-frequency peak of the vacf spectra $f(\omega)$

5. Conclusions

At the smallest accessible q-vectors, the coherent dynamic structure factor of the oxygen motion in low-density water gives a clear indication for the presence of two distinct collective modes. This is in agreement with the observations of Rahman and Stillinger and supports the subsequent interpretation of light- and neutron-scattering experiments, according to which the low-frequency mode is a remnant of the "ordinary" sound and the high-frequency mode is a collective excitation within the H-bond network. This picture is reinforced by the damping behavior of the two Brillouin-peaks.

Whereas the LF peak vanishes at $q \approx 0.5$ Å^{-1} ($q \cdot \sigma \approx 1.4$, where $\sigma = 2.8$ Å is the position of the first peak in the oxygen pair distribution function), the HF peak persists up to about 1.7 Å^{-1} ($q\sigma \approx 4.8$). In previous simulations and scattering experiments Brillouin-lines had been observed up to $q\sigma \leq 0.5$ (for hard spheres) and $q\sigma \leq 4.0$ (for liquid rubidium). Thus the limit of observability for the LF peak is well within the usual bounds, but is situated beyond this range for the HF excitation. Additionally, the damping of the HF peak does not increase, when the density is decreased, as one would expect from hydrodynamics in view of the changes in mobility (viscosity). On the contrary, this mode becomes less damped, i.e. more solid-like due to the strengthening of the H-bond network.

After having discussed now the existence of two distinct modes, we have to be aware of the calculations of Ricci et al. [15] which suggest the existence of even a *third* independent mode. This one has to be attributed to correlations in the hindered rotations of the molecules ("collective librations"). A corresponding peak was observed in the spectrum

of the hydrogen motions. Therefore, in a preliminary study we calculated also the intermediate scattering function of the hydrogens in the low-q region. We found nearly perfect agreement with the oxygen functions Fig. 1a–c. Only at very short times ($t \leq 0.02$ ps, which corresponds to the initial librational decay of the reorientation correlation functions of the water molecules [12, 18]), the intermediate scattering functions deviated from each other, as it has been observed by Ricci et al. Further evaluation of our data along the lines of these authors has to be done. To substantiate the assignment of various mechanisms to the observed peaks in the spectra of the collective motions, it would also be helpful to vary systematically parameters like the hydrogen mass. Finally, we suggest using larger systems, to investigate the low-q limit of the high-frequency modes.

We thank the computer-centers of RWTH Aachen and Universität Dortmund. Financial support of the "Fonds der Chemischen Industrie" is gratefully acknowledged.

References

[1] J.-P. Hansen and I. R. McDonald, Theory of Simple Liquids, 2nd edition, Academic Press, London 1986.
[2] J.-P. Boon and S. Yip, Molecular Hydrodynamics, McGraw-Hill, New York 1980.
[3] N. E. Cusack, The Physics of Structurally Disordered Matter, Adam Hilger, Bristol 1987.
[4] J. R. D. Copley and J. W. Rowe, Phys. Rev. Lett. *32*, 49 (1974), and Phys. Rev. *A9*, 1656 (1974).
[5] O. Söderström, J. R. D. Copley, J. B. Suck, and B. Dorner, J. Phys. *F10*, L151 (1980).
[6] H. G. Bell, H. Moeller-Wenghoffer, A. Kollmar, R. Stockmeyer, T. Springer, and H. Stiller, Phys. Rev. *A11*, 316 (1975).
[7] A. Rahman and F. H. Stillinger, Phys. Rev. *A10*, 368 (1974).
[8] J. Rouch, C. C. Lai, and S. H. Chen, J. Chem. Phys. *65*, 4016 (1976); J. Teixeira and J. Leblond, J. Phys. (Paris), Lett. *39*, L83 (1978).
[9] J. Teixeira, M.-C. Bellissent-Funel, S. H. Chen, and B. Dorner, Phys. Rev. Lett. *54*, 2681 (1985).
[10] L. Bosio, J. Teixeira, and H. E. Stanley, Phys. Rev. Lett. *46*, 597 (1981).
[11] A. Geiger and H. E. Stanley, Phys. Rev. Lett. *49*, 1749 (1982).
[12] R. W. Impey, P. A. Madden, and I. R. McDonald, Mol. Phys. *46*, 513 (1982).
[13] M. Wojcik and E. Clementi, J. Chem. Phys. *85*, 6085 (1986).
[14] M. A. Ricci, D. Rocca, G. Ruocco, and R. Vallauri, Phys. Rev. Lett. *61*, 1958 (1988).
[15] M. A. Ricci, D. Rocca, G. Ruocco, and R. Vallauri, preprint.
[16] J. Bosse, G. Jacucci, M. Ronchetti, and W. Schirmacher, Phys. Rev. Lett. *57*, 3277 (1986).
[17] A. Geiger, F. H. Stillinger, and A. Rahman, J. Chem. Phys. *70*, 4185 (1979).
[18] A. Geiger and P. Mausbach, in: "Hydrogen-bonded Liquids", edited by J. C. Dore, NATO ASI Series, in press.
[19] H. E. Stanley and J. Teixeira, J. Chem. Phys. *73*, 3404 (1980).
[20] H. E. Stanley, R. L. Blumberg, A. Geiger, P. Mausbach, and J. Teixeira, J. Phys. (Paris) *45*, C7-3 (1984).
[21] E. W. Lang and H.-D. Lüdemann, Angew. Chem. Int. Ed. Eng. *21*, 315 (1982); C. A. Angell, Ann. Rev. Phys. Chem. *34*, 593 (1983).
[22] A. Geiger, P. Mausbach, J. Schnitker, R. L. Blumberg, and H. E. Stanley, J. Phys. (Paris) *45*, C7-13 (1984).
[23] A. Geiger, P. Mausbach, and J. Schnitker, in: "Water and Aqueous Solutions", edited by G. W. Neilson and J. E. Enderby, Adam Hilger, Bristol 1986.
[24] H. G. Hertz and C. Rädle, Z. Phys. Chem. Neue Folge *68*, 324 (1969).
[25] R. J. Speedy, J. Phys. Chem. *86*, 982 and 3002 (1982).
[26] J. C. Dore, in: "Water Science Reviews", Vol. 1, edited by F. Franks, University Press, Cambridge 1985.
[27] P. A. Giguère, J. Chem. Phys. *87*, 4835 (1987).
[28] D. E. Polk, J. Non-Cryst. Solids *5*, 365 (1971).
[29] N. N. Medvedev and A. Geiger, to be published.
[30] O. Steinhauser, Mol. Phys. *45*, 335 (1982).
[31] D. Fincham and D. M. Heyes, Adv. Chem. Phys. *63*, 493 (1985).
[32] G. R. Kneller, Ph. D. thesis TWTH Aachen 1988 and report Nr. 2215, KFA Jülich; G. R. Kneller and A. Geiger, Mol. Phys. *68*, 487 (1989).
[33] H. Wormeester, A. G. B. M. Sasse, and A. van Silfhout, Comput. Phys. Commun. *52*, 19 (1988).
[34] S. Krishnamurthy, R. Bansil, and J. Wiafe-Akente, J. Chem. Phys. *79*, 5863 (1983).
[35] P. Mausbach, J. Schnitker, A. Geiger, and H. E. Stanley, in: "Rarified gas dynamics", edited by H. Oguchi, University of Tokyo Press 1984.

Presented at the Joint Discussion Meeting of the Deutsche Bunsen-Gesellschaft für Physikalische Chemie, Associazione Italiana di Chimica Fisica, Faraday Division of the Royal Society of Chemistry, Société Française de Chimie, Division de Chimie Physique, "Transport Processes in Fluids and in Mobile Phases" Aachen, September 25th to 27th, 1989

E 7255

The Molecular Dynamics of Adsorbed Hydrocarbons

S. Leggetter and D. J. Tildesley

Department of Chemistry, The University, Southampton S09 5NH U.K.

Adsorption / Statistical Mechanics / Surfaces

The molecular dynamics simulation technique has been used to study the adsorption of hydrocarbons on a structured graphite surface. Simulations were performed on a united atom model of butane at 282 K and surface coverages of 22.3 Å^2/molecule and 32 Å^2/molecule. One simulation of decane was performed at 291 K and a surface coverage of 85.6 Å^2/molecule. We report in-plane and out-of-plane velocity autocorrelation functions and the surface diffusion coefficients, angular velocity and the reorientational correlation functions and the time correlation functions associated with the conformational dynamics of these flexible molecules.

1. Introduction

Physically adsorbed monolayers of atoms and molecules adsorbed on graphite have been studied by theory and experiment over the last fifteen years [1, 2]. Computer simulation has played a central role in these developments. Comparison of simulation with experiment allows us to adjust